THE TIME-TEMPERATURE-TRANSFORMATION BEHAVIOR OF ALLOY 706

Karl A. Heck

Inco Alloys International, Inc.
P.O. Box 1958
Huntington, WV 25720

Abstract

The isothermal time-temperature-transformation behavior of wrought, triple melted (VIM-ESR-VAR) and homogenized INCONEL® alloy 706 was characterized by X-ray diffraction, SEM/EDX, and optical metallographic techniques. Microstructural features, including phase compositions, morphologies, and crystal structures are discussed. Alloy 706 is an age-hardenable superalloy strengthened by γ' and γ'' precipitation at lower temperatures. The propensity for the alloy to form η at higher temperatures distinguishes alloy 706 T-T-T behavior from that of the well documented INCONEL® alloy 718. The effect of differing Nb-Ti-Al ratios and Fe content on the physical metallurgy of Nb-Containing superalloys is discussed.

Introduction

INCONEL® alloy 706 was developed during the late 1960's to satisfy requirements for very large forged gas turbine components. Alloy 706 evolved from the INCONEL® alloy 718 composition. Nickel and hardener content were lowered to ease forgeability and reduce tendency for macrosegregation within large cross-sections. Industry experience and technical studies on alloy 706 prior to 1990 centered on double melted (VIM-VAR) material. More recently, stringent requirements on larger ingots processed into rotating components resulted in development of triple melt processes to produce uniform final ingot structure and very low sulfur content(1). In this paper, an updated time-temperature-transformation (T-T-T) characterization is presented.

Procedure:

A 51mm square bar cut from a triple melted (VIM-ESR-VAR) and homogenized 914mm diameter ingot was heated to 1121°C and rolled to 17mm diameter round. Composition is shown in Table 1. This hot working temperature was used to produce the relatively coarse grain structure expected in a large forging. Pieces from half of the bar were annealed at 1121°C/1h, then oil quenched (OC). Pieces from the other half were annealed at 982°C, then air cooled (AC). These temperatures are commonly used for hot working, reheating, and annealing.

Superalloys 718, 625, 706 and Various Derivatives
Edited by E.A. Loria
The Minerals, Metals & Materials Society, 1994

Quench methods were chosen to minimize precipitation and strain induced aging after the anneals(2). Both sets of samples were isothermally heat treated in increments of 55°C from 538°C to 1093°C and intervals of 6 minutes, 1, 10 and 100 hours followed by a water quench.

Table 1. Composition (wgt. %)

Ni	Fe	Cr	Nb	Ti	Al	C	Si	N	S
41.8	36.9	16.0	3.02	1.65	0.19	0.01	0.05	0.003	0.001

Samples were mounted and examined optically and by SEM in longitudinal and transverse orientation using 1% aluminum sulfate + 1% citric acid in water (citric solution) or phosphoric acid (electrolytic) etchants. X-ray diffraction of particles extracted by the citric solution, and 20% HCl + 1.5% tartaric acid in methanol was performed using Cu radiation.

Results and Discussion

Experimental Techniques:

Electrochemical extraction and etching of alloy 706 is fairly straightforward. Swab etchants, such as Kalling's reagent and 7-acids etch, and electrolytic 10% HCl in methanol or CrO_3 saturated water worked well to show general grain structure. To reveal precipitated phases, electrolytic etching in 90 parts H_3PO_4 /10 parts water produced the most consistent results. This solution etches grain boundaries sensitized by precipitates, but will not etch clean boundaries.

The citric solution extracted and etched (in relief) γ', γ'', and η phases very well, but was poor for isolation of carbides and nitrides and did not etch grain boundaries. Samples dissolved in this solution required reactivation by repeated ultrasonic agitation in methanol. The HCl + methanol solution was effective for extracting MC, TiN, and A_2B Laves, but extracted no γ' and only a very small proportion of total γ'' and η.

Annealed Samples:

Material in both annealed conditions contained approximately 0.15 weight percent blocky M(C,N) [M = Nb, Ti] and TiN particles that formed during solidification. Most of these particles are gray in color, and have an MC crystal structure. Gold colored TiN is visible only at the center of larger blocky particles, and is much less frequent than M(C,N). The outer edges of these cored particles are gray, indicating enrichment in carbon and Nb. X-ray diffraction showed small amounts of the hexagonally structured TiN relative to M(C,N). $Ti_4C_2S_2$, a phase that can contribute to lower transverse ductility if present in stringer or pancake morphology (1), was not found.

1121°C/1 Hour Anneal (Figure 1):

All precipitates are in solution, and grain size is a relatively coarse ASTM #1. This full solution anneal makes C available for MC (M = Nb,Ti) precipitation in existing grain boundaries below 1080°C. This precipitation, not reported in previous work on an older version of alloy 706 annealed at 1093°C(3), forms as fine discrete particles in grain boundaries above 816°C, and is coarser and more widely spaced above the η solvus. After long times at 927°C, a very fine MC precipitation occurs intragranularly in advance of intragranular η. Grain boundary precipitation has a feathery, film-like morphology at and below 760°C, and is not observed after 100 hours at 816°C. It is known that the presence of films in existing boundaries can reduce ductility and impact strength. As seen in Figure 1 (c and d), heat treatment of 1121°C annealed material produces uniform intragranular η precipitation.

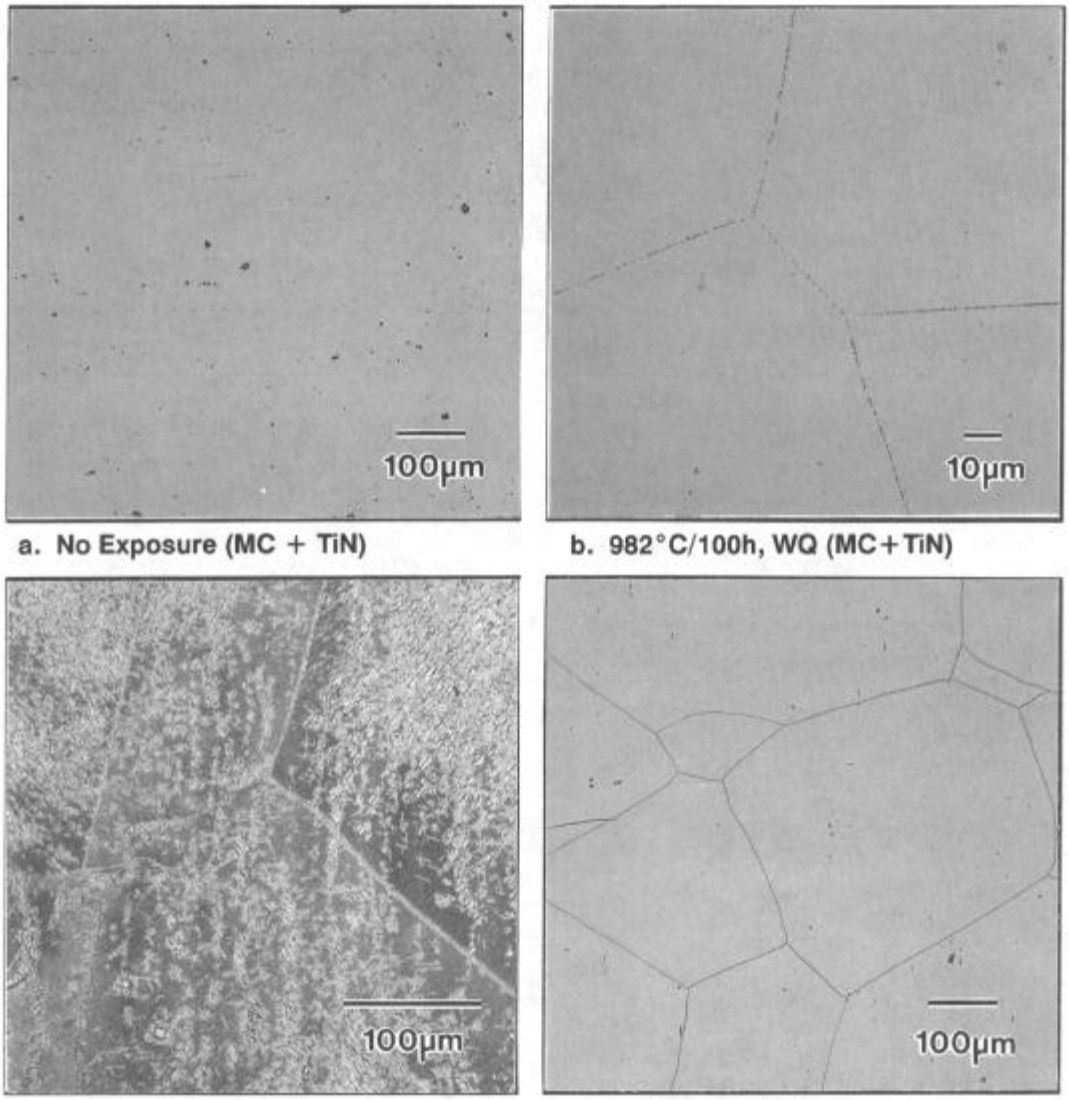

a. No Exposure (MC + TiN)

b. 982°C/100h, WQ (MC+TiN)

c. 816°C/100h,WQ ($\gamma'+\gamma''+\eta+A_2B$)

d. 704°C/10h, WQ (MC+TiN + γ')

Figure 1. 1121°C/1h, OC + Isothermal Heat Treatment Shown (H_3PO_4 etchant)

982°C/1 Hour Anneal (Figure 2):

This anneal resulted in a grain size of ASTM #3. Very fine MC particles delineate prior warm worked grain boundaries in a "ghost grain" structure. These fine particles are best revealed by using the electrolytic H_3PO_4 etchant. (The particle network is later shown to be associated with non-uniformly nucleated η, and non-uniformly precipitated of carbides). The prior particle structure appears stable at high temperature, as additional MC does not precipitate in existing grain boundaries of samples held above 982°C for longer periods of time (Figure 2b). Additional MC precipitation occurs below 982°C. The particles almost completely dissolve in one hour at 1080°C, and are absent after one hour at 1093°C. (Carbonitride particles present from solidification do not go into solution). Eta solutions between 927°C and 982°C.

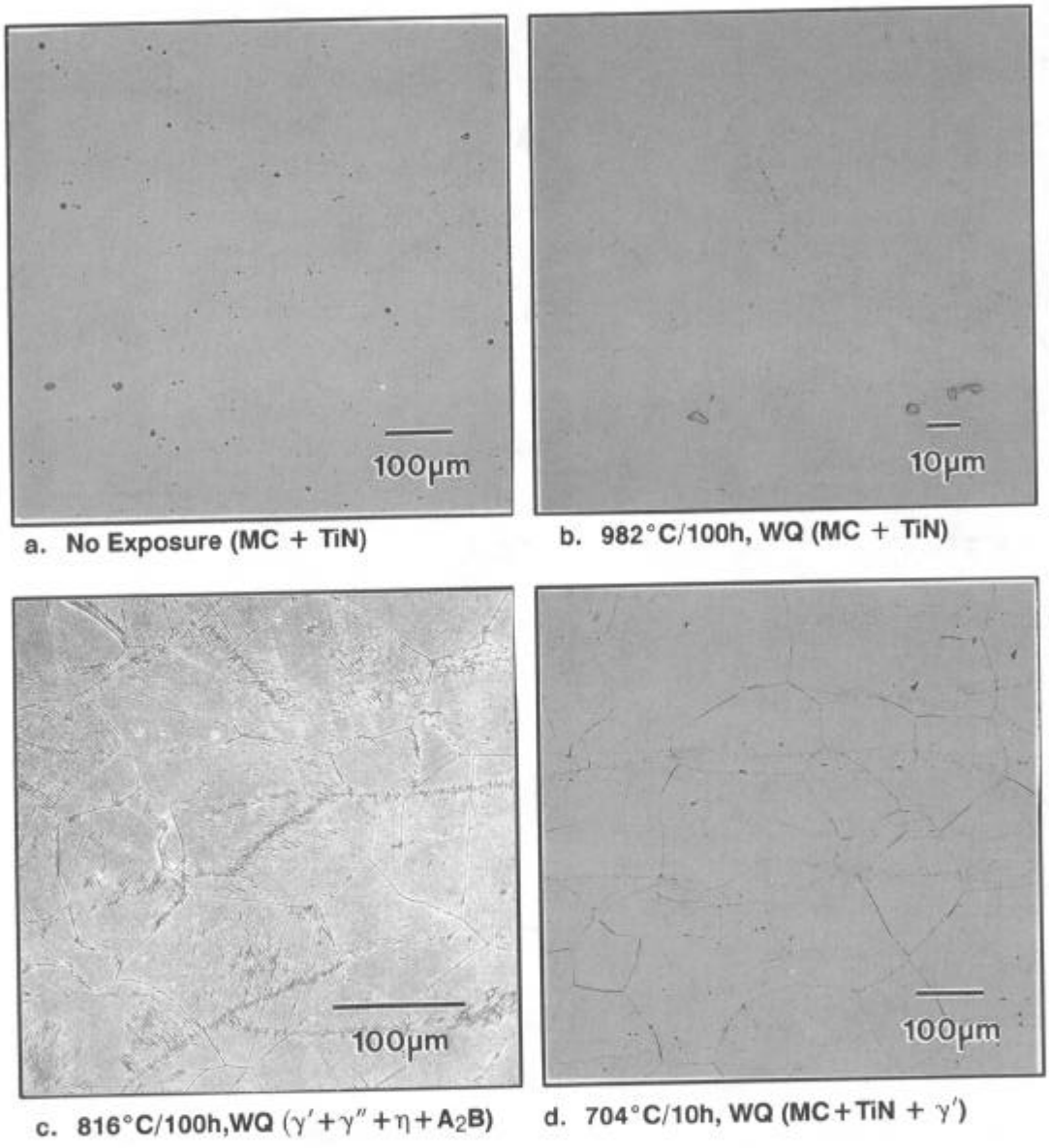

a. No Exposure (MC + TiN)

b. 982°C/100h, WQ (MC + TiN)

c. 816°C/100h,WQ ($\gamma' + \gamma'' + \eta + A_2B$)

d. 704°C/10h, WQ (MC + TiN + γ')

Figure 2. 982°C/1h, AC + Isothermal Heat Treatment, WQ(H_3PO_4 etchant)

Figure 2c shows η nucleated at 816°C in a cellular network elongated parallel to the direction of prior warm work. At lower temperatures (below 816°C), continuous MC precipitate forms in grain boundaries between prior particle regions. Grain boundaries in the prior particle regions remain clean. This shows that thermomechanical processing (TMP) can be used to control grain boundary precipitation during subsequent heat treatment. A closer view of this phenomenon is shown in Figure 3. The use of colder final hot working temperature combined with the low temperature anneal would result in a more uniform dispersion of MC and a finer grain structure (larger grain boundary area). This process should minimize the formation of the continuous films and non-uniform η.

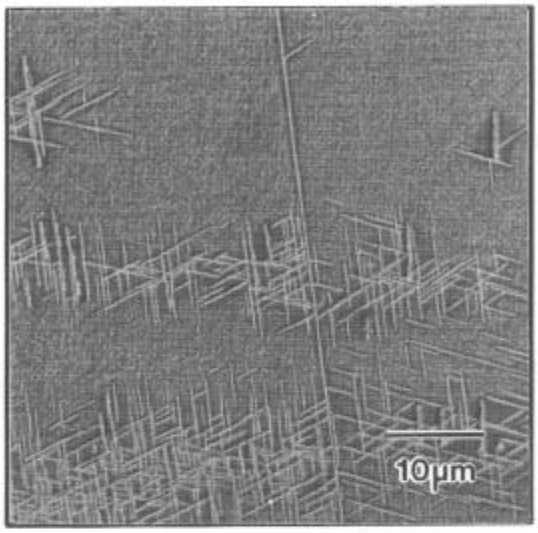

a. 816°C/100h, WQ
longitudinal cross-section showing non-uniform $\eta + \gamma''$
(SEM, citric acid solution)

b. 816°C/100h, WQ
Surface of extracted sample showing η platelets outlining prior warm-worked structures.
(SEM citric acid solution)

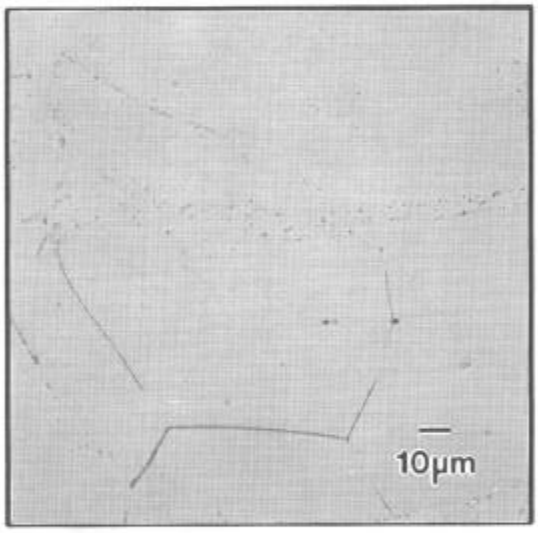

c. 704°C/100h, WQ
Sample showing absence of grain boundary films in regions containing prior boundary carbide particles.
(optical, H_3PO_4 etchant)

Figure 3.
Higher magnification micrographs showing non-uniform precipitation in material aged after an 982°C/1h, AC anneal.

Precipitation Treatments:

Hardness:

Hardness test results for 982°C annealed then aged samples are shown in Figure 4. (1121°C annealed material showed similar results). Aging response is accelerated between 760°C and 816°C, but peak hardness occurs at longer times between 704°C and 760°C. The T-T-T curves in Figure 5 show that increases in hardness correlate with precipitation of γ' and γ''. The highest isothermally generated hardnesses are associated with greater amounts of $\gamma' + \gamma''$ and the onset of η precipitation. In general, hardness decreases with increasing amounts of η, although slight hardening relative to the annealed state occurs where η (especially) and A_2B precipitation thoroughly transform grains to Widmanstätten structure.

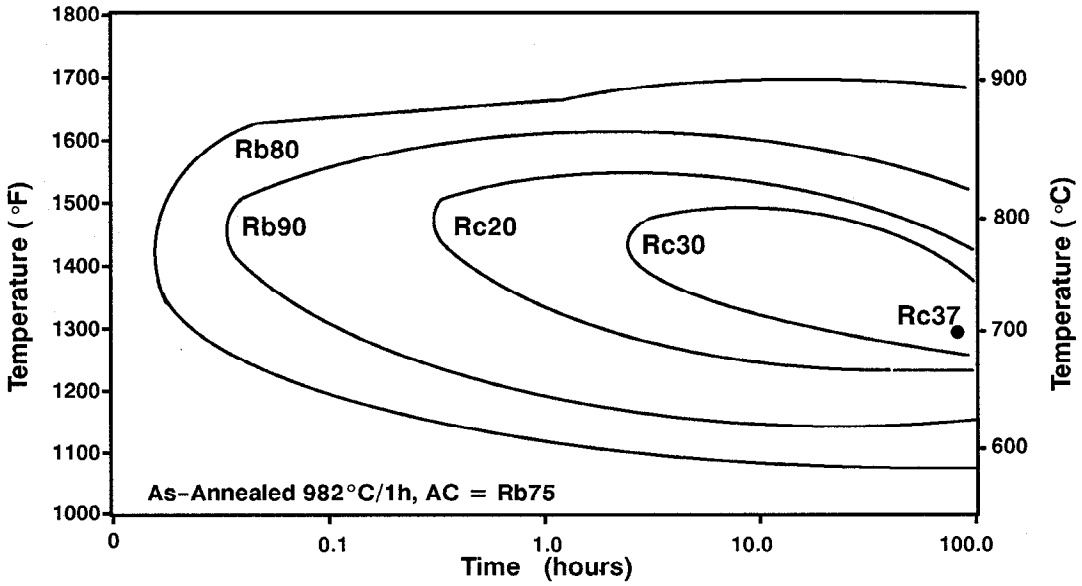

Figure 4: Time-Temperature-Hardness Diagram

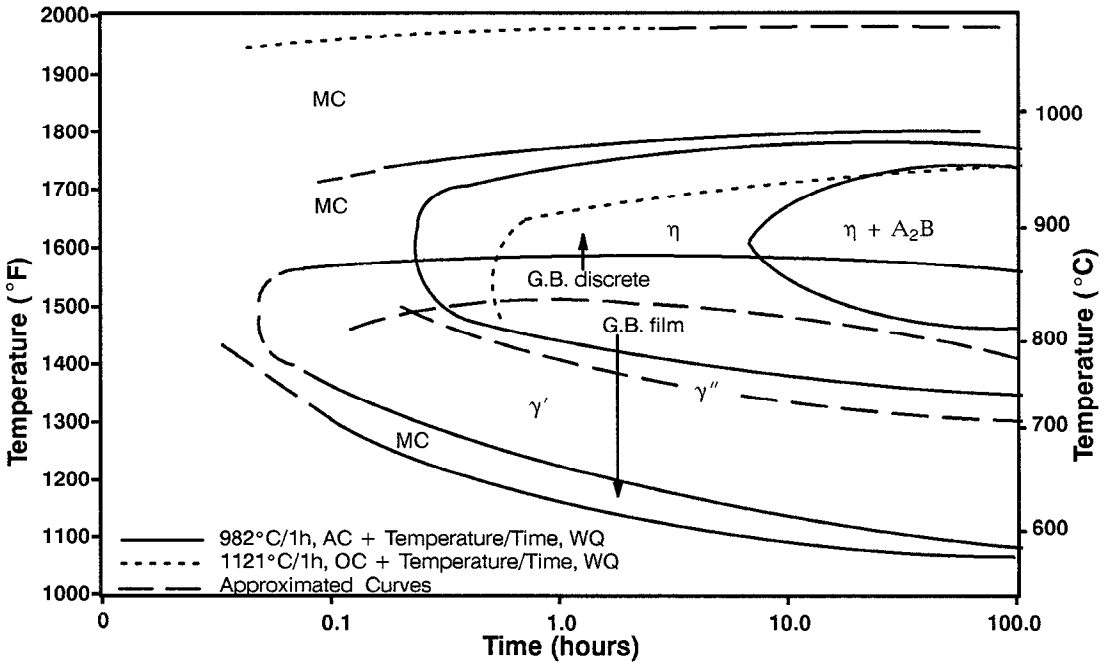

Figure 5. Isothermal T-T-T Diagram for Alloy 706

Precipitated Phases:

The two annealed conditions exhibit T-T-T behavior shown in Figure 5, which is similar to previous reports (4-7). The precipitation curves for MC are correlated with the upper temperature range of η precipitation (shifted depending on anneal condition). Phases indicated on the T-T-T diagram have compositions and crystal structures described in Figure 6.

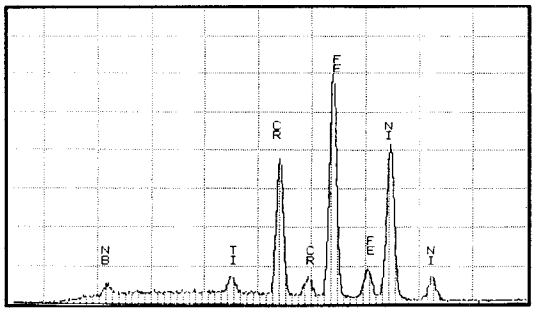

a. Annealed matrix
XRD pattern similar to
JCPDS #31-619 (Austenite)

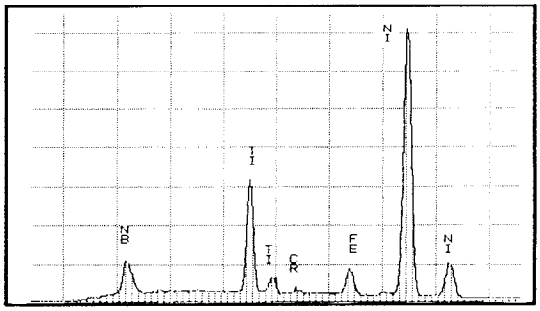

d. Eta η
XRD pattern similar to
JCPDS #23-1275 ($Ni_3(Ti_{.97}Nb_{.03})$

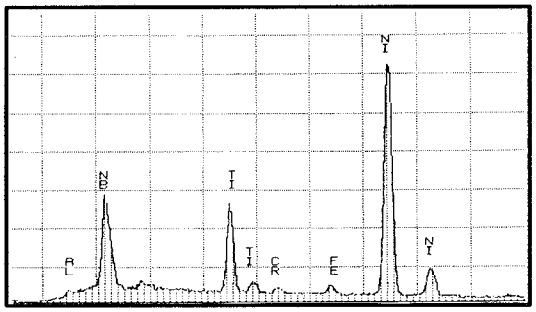

b. Gamma Prime (γ')
XRD pattern similar to
JCPDS #19-35 ($Ni_3(Al,Ti)$)

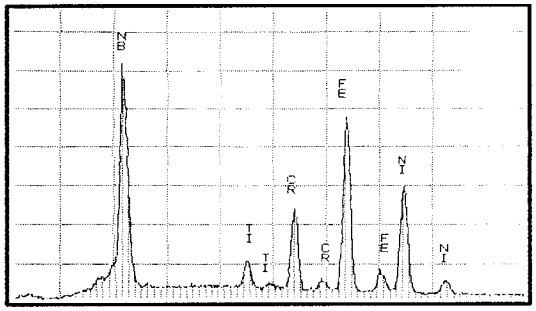

e. Laves (A_2B)
XRD pattern similar to
JCPDS #17-908 (Fe_2 Nb)

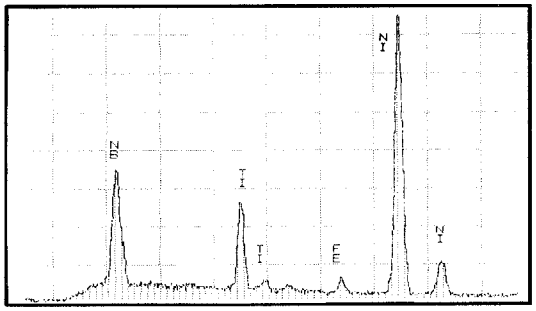

c. Gamma Double Prime (γ'')
XRD pattern similar to
JCPDS #18-893 (Ni_3Ta)

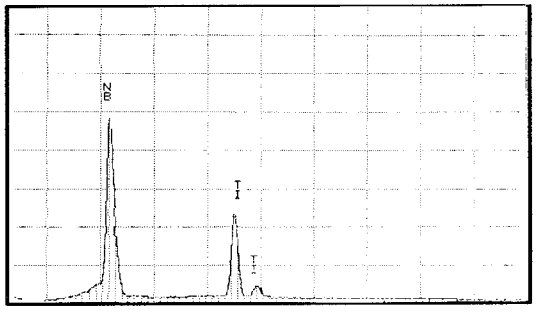

f. (Nb,Ti) C (MC Carbide)
XRD pattern similar to
JCPDS #38-1364 (NbC)

(Not shown: TiN, JCPDS #38-1420)

Figure 6: Phase Compositions (EDX spectra of extracted precipitates)

MC Carbide:

This Nb and Ti rich MC carbide can form as a dispersion of very fine particles during processing, or can precipitate in grain boundaries after a full solution anneal (Figure 7). The carbides are cubic (a=4.43Å). Possible small amounts of $M_{23}C_6$ or NbN occasionally appeared in diffraction patterns with MC. Phase analyses in earlier studies(3) did not reveal this precipitate (other than carbonitride particles from solidification). The composition of older production heats (i.e., higher N and Si) may have favored a lower carbon solubility thus stabilizing high temperature carbides. These carbides, formed during hot working and annealing, inhibit additional carbide precipitation, but accelerate η precipitation during aging treatments.

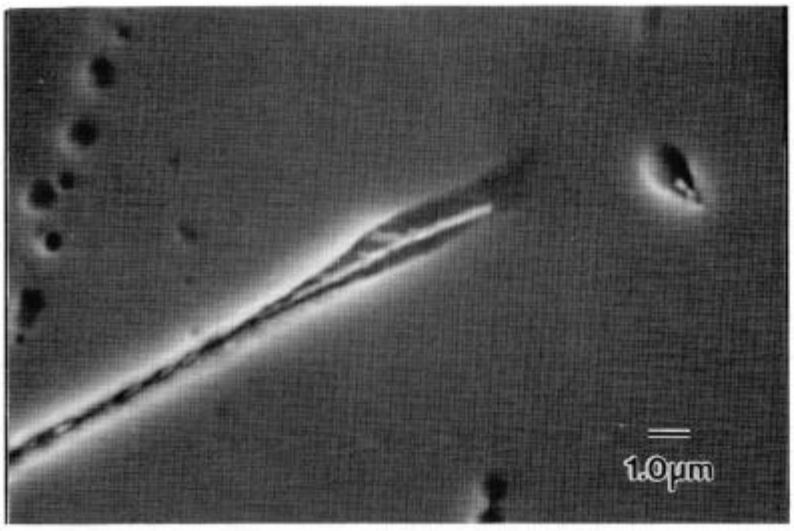

Figure 7: Grain Boundary MC Carbide Precipitated after 1121°C/1h, OC +982°C/100 h, WQ (SEM, H_3PO_4 etchant)

Gamma Prime (γ'):

Gamma prime is the predominate age hardening phase formed by isothermal heat treatments at and below 704°C. γ' precipitates before γ'' at 760°C. Based upon $Ni_3(Ti,Nb)$, the fine spherical particles are ordered $L1_2$ (a=3.57Å). In this material, γ' solutioned in one hour at 871°C, and between 816°C and 871°C at longer times. This solvus is slightly lower than previously reported (2), probably due to differences in Al content.

Gamma Double Prime (γ''):

Gamma double prime is the predominate age hardening phase formed by heat treatments at 760°C and 816°C. The small disk shaped precipitates are richer in Nb than γ', and have an ordered BCT crystal structure. The presence of γ'' coincides with the onset of Ti-rich η precipitation. Gamma double prime appears to transform to, or solution and reprecipitate as η simultaneously with γ'.

Eta Phase (η):

Eta phase, Ni_3 (Ti,Nb) with a hexagonal DO_{24} structure, forms as small platelets in grain boundaries (Figure 8) and as very thin but broad platelets within grains. Eta coarsens at the expense of γ' and γ'' between approximately 760°C and 871°C (Figure 9). In cross-section, the platelets appear as needles (Figure 10). Eta nucleates uniformly within grains after a 1121°C anneal, but non-uniformly when starting with the 982°C anneal condition. This appears related to remnant substructures outlined by fine MC particles. It was not determined whether this effect is due to crystal defect structure or local matrix composition variation introduced by the prior boundary precipitates. The latter seems most likely since this occurs in a fully recrystallized grain structure, and carbide formation appears to influence the η solvus. Delta phase (δ-orthorhombic Ni_3Nb) was not conclusively isolated in this study.

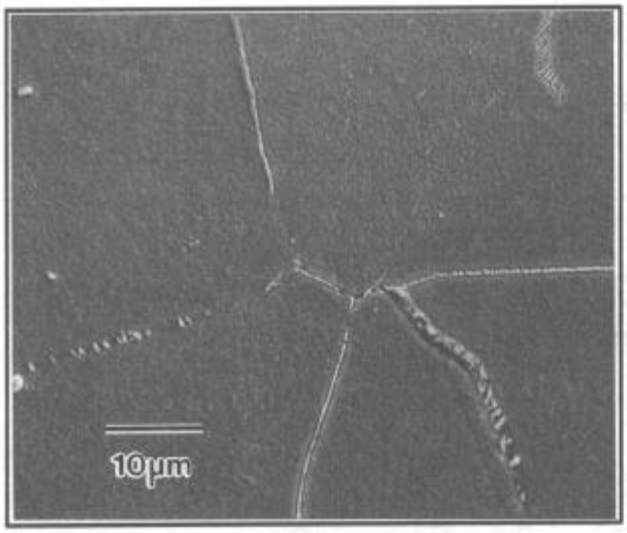

Figure 8:

982°C/1h, AC +760°C/100h,WQ. Platelets in grain boundaries are η, continuous phase is MC. Grain interiors contain γ′+γ″and some small η platelets.
(SEM, citric acid solution)

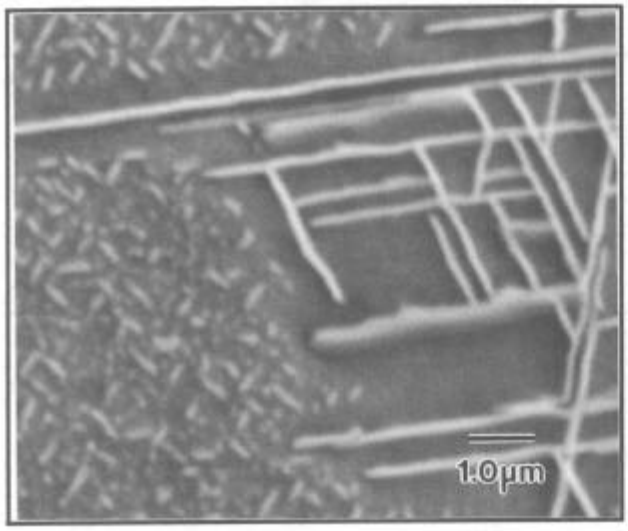

Figure 9:

982°C/1h,AC+816°C/100h,WQ showing γ′ , γ″ and η . Note the absence of γ′ (small spheres) and γ″(small platelets) near larger η platelets.
(SEM, citric acid solution)

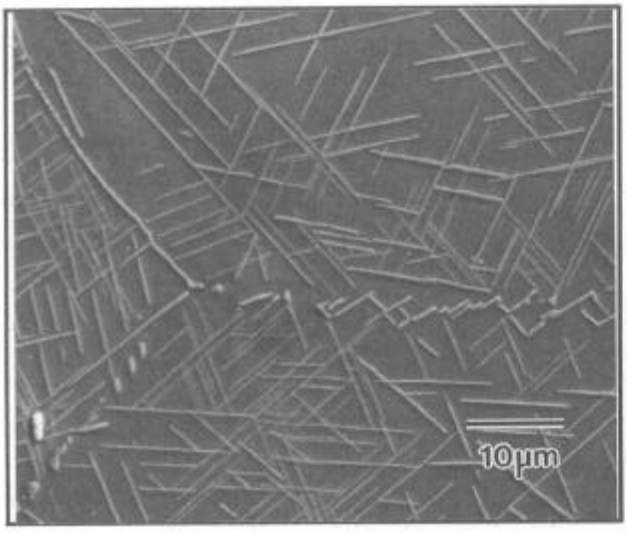

Figure 10:

Eta precipitates after 982°C/1h, AC +871°C/100h, WQ.
γ′ and γ″ are in solution and/or transformed to η.
(SEM, citric acid solution)

Laves Phase (A_2B):

A precipitated Laves phase based on Fe_2Nb was found in greatest abundance after long heat treatments at 871°C–927°C. This blocky and platelet shaped precipitate has morphologies similar to grain boundary η, although coarser (labelled "L" in Figure 11). The material in this study appears to have formed less Laves than reported in earlier work, probably due to lower Si content in current production which would lower N_V.

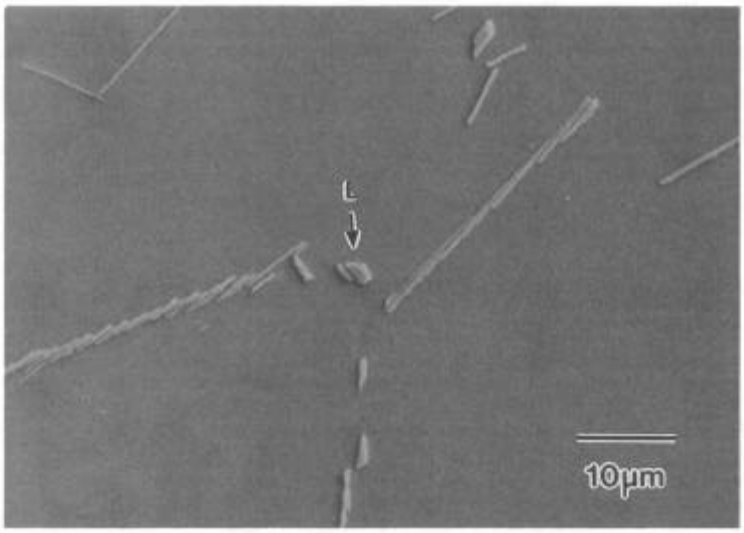

Figure 11: 982°C/1h, AC + 927°C/100h, WQ showing thin η platelets and blockier A_2B particles. (SEM, citric acid solution)

Commercial Heat Treatments:

A typical alloy 706 commercial aging treatment is 718°C/8 hours, furnace cooled at 55°C/hour to 621°C/8 hours, air cooled. This type of treatment provides high strength due to the fine scale of γ''/γ' precipitation at the higher temperature step, combined with stabilization and additional fine precipitation during the furnace cool and lower temperature hold. This practice achieves high strength in a much shorter period of time, and with less likelihood for overaging to intragranular η than if a long isothermal heat treatment was used. Where increased stress rupture capability is desired, a heat treat step of 843°C for 3 hours is inserted between the anneal and aging step. This treatment step, near the γ''/γ' solvus, precipitates discontinuous grain boundary η that enhances high temperature notch ductility (Figure 12). This T-T-T work suggests that the 843°C step may also minimize the potential for grain boundary precipitation in continuous morphologies during lower temperature aging steps.

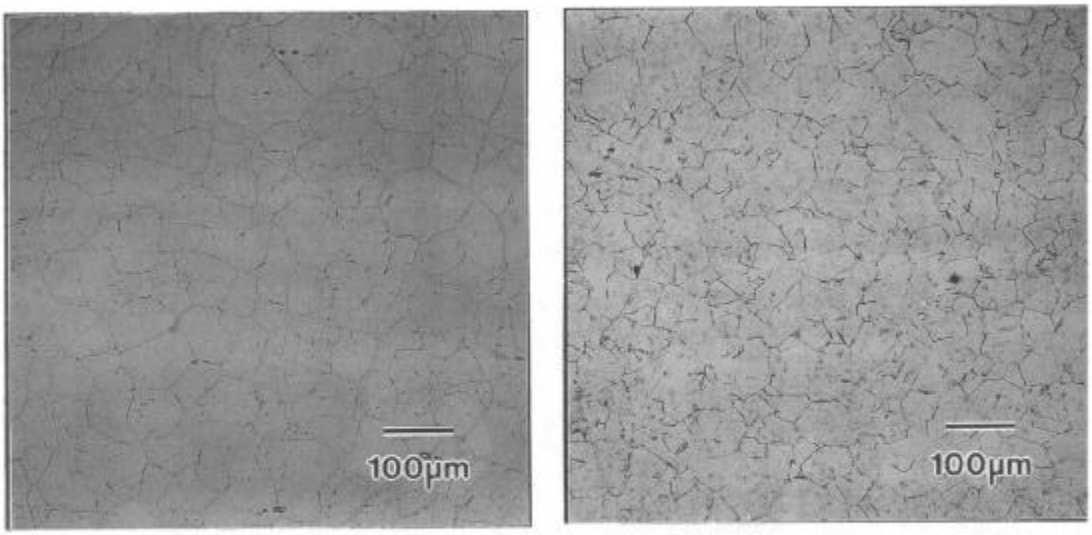

a.982°C/1h, AC + 718°C/8h, FC (55°C/h) to 621°C/8h, AC

b. 982°C/1h, AC + 843°C/3h, AC + 718°C/8h, FC (55°C/h) to 621°C/8h, AC

Figure 12. Triple melted and forged alloy 706 showing grain boundary precipitation from 843°C/3h, AC step for improved stress rupture behavior. (optical, 7-acids etchant)

Conclusions and Summary:

Alloy 706 is a nickel based superalloy age-hardenable by the precipitation of Ni_3 (Ti,Nb) γ' and Ni_3(Nb,Ti) γ''. The predominant stable overaged constituent is Ni_3 (Ti,Nb) η. An Fe_2Nb-type Laves phase forms after longer times in the η precipitation range. (Nb,Ti)C based grain boundary carbide forms over a broad temperature range. Prior TMP and annealing temperatures affect the distribution of precipitated carbides and η phase. Carbide precipitation interacts with η formation.

Care was taken in this study to produce a heavily wrought, homogeneous microstructure of triple melted alloy 706. It should be recognized that less chemically homogeneous structures having received less warm work may have localized precipitation responses different from those reported here. Chemical inhomogeneities are expected to shift T-T-T curves to shorter times in solute rich areas (such as interdendritic regions carried over from cast structure), thus promoting non-uniform phase precipitation. In addition, relatively minor differences in alloy 706 aluminum content affect the stability of γ' versus γ''(8). By similar argument, prior precipitation of a phase richer in Ti (such as η) would likely enhance localized precipitation of Nb-rich γ'' (and possibly δ). Further, strain induced η precipitation will occur if mini-grain processing is used for grain refinement (9). Therefore, the precipitation responses encountered during the multi-step heat treatment of large commercial parts may differ from the isothermal transformations observed in this controlled study.

References

1. P. W. Schilke, J. J. Pepe, R. C. Schwant, "Alloy 706 Metallurgy and Turbine Wheel Application," International Special Emphasis Symposium on Superalloys 718, 625, 706 and Derivatives, TMS, Pittsburgh, PA, June 1994.

2. J. Moll, G. Maniar, D. Muzyka, "Heat Treatment of 706 Alloy for Optimum 1200°F Stress-Rupture Properties", Met. Trans., Vol. 2, 1971, pp. 2153-2160.

3. H. L. Eiselstein, "Properties of INCONEL alloy 706", ASM T.R. C 70-9.5. Presented at Materials Engineering Exposition & Congress 19-22 October, 1970, Cleveland, OH.

4. L. Remy, "Precipitation Behaviour and Creep Rupture of 706 Type Alloys", Materials Science and Engineering, 38, 1979, pp. 227-239.

5. J. Moll, G. Maniar, D. Muzyka, "The Microstructure of 706, a New Fe-Ni-Base Superalloy", Met. Trans., Vol. 2, 1971, pp. 2143-2151.

6. W. L. Bell, et al, "Microstructural Changes in Ion-Irradiated Commercial Alloys", Irradiation Effects on the Microstructure and Properties of Metals, ASTM STP 611, ASTM, 1976, pp. 353-369.

7. L. E. Thomas, "The Stability of γ' and γ'' in INCONEL alloy 706 Under Neutron Radiation", Conference: Phase Stability During Irradiation, TMS/AIME, Pittsburgh, PA., Oct 5-9, 1980, pp. 237-255,.

8. E. L. Raymond, D. A. Wells, "Effects of Aluminum Content and Heat Treatment on Gamma Prime Structure and Yield Strength of INCONEL Nickel-Chromium Alloy 706", Superalloys, NITS, Springfield, VA, 1972, pp. N1-N21.

9. D. R. Muzyka, G. N. Maniar, "Microstructure Approach to Property Optimization in Wrought Superalloys", Metallography - A Practical Tool for Correlating the Structure and Properties of Materials, ASTM STP 557, ASTM, 1974, pp. 198-219.